A hybrid PRF/T1 pulse sequence for rapid, simultaneous temperature tracking in soft and adipose tissues

N. Todd[1], and D. L. Parker[2]

[1]Physics, University of Utah, Salt Lake City, UT, United States, [2]Radiology, University of Utah

INTRODUCTION

For MR guided thermal therapies to be fully safe and effective, it is necessary to be able to monitor temperatures in both soft (non-adipose) and fatty tissues. The widely used proton resonance frequency (PRF) technique can adequately measure temperature changes in soft tissue, but rapid, accurate temperature measurements in fatty tissue remains an unsolved problem in MR. The lack of a temperature dependent chemical shift coefficient for hydrogen in methyl and methylene groups confounds the PRF technique, but fat still has a temperature dependent longitudinal relaxation time, T1. In order to simultaneously track temperature changes in soft and fatty tissue, we have developed a hybrid PRF/T1 pulse sequence. This is the standard PRF gradient echo sequence acquired with variable flip angles. The phase information from the sequence can be used to create PRF temperature maps after every scan, and T1 information can be derived from as few as two consecutive scans at different flip angles. In this way, temperature can be monitored in soft tissue without loss of temporal resolution or accuracy and temperature in fatty tissues can be tracked with a temporal resolution that is only half to a third that of the PRF method.

METHODS

The hybrid PRF/T1 pulse sequence consists of a standard spoiled gradient echo sequence run consecutively with two or more different flip angles. For the initial experiment, the parameters were set to: TR = 36msec, TE = 6msec, 1.5x1.5x3.0mm^3 resolution, and flip angles = 20°, 50°, and 70°. Using a Siemens TIM Trio 3T MR scanner (Siemens Medical Solutions, Erlangen, Germany), 3 slices could be scanned every 4.5 seconds.

PRF temperature information is extracted in the normal way, using the fact that temperature change is proportional to the phase difference of consecutive images[2]. The phase information can be gathered after every run of the gradient echo sequence.

To extract the T1 information, the sequence must be run at least twice with varying flip angles. In a gradient echo sequence, the signal magnitude is dependent on T1 and flip angle, α, in the following way:

$$S = M_0 \frac{(1-E_1)\sin\alpha}{1-E_1\cos\alpha} E_2 \quad \text{where } E_1 = \exp(-T_R/T_1) \text{ and } E_2 = \exp(-T_E/T_2^*) \qquad [1]$$

Eq. [1] can be linearized and T1 extracted from the slope of the line, *m*, as follows[2]:

$$\frac{S}{\sin\alpha} = \frac{S}{\tan\alpha} E_1 + M_0(1-E_1)E_2 \quad \text{and} \quad T_1 = -T_R/\ln(m) \qquad [2]$$

In order to optimize the accuracy of the T1 measurement, both the Ernst angle and a large dynamic range must be kept in mind. Flip angles near the Ernst angle will provide a stronger signal while choosing two flip angles far apart will help to reduce error in the linear fit.

B1 field inhomogeneity will cause actual flip angles through out the volume to be different than what was specified in the pulse sequence. To correct this effect, two spin echo scans with two sets of angles were acquired: θ_1-τ-2θ_1-τ, and θ_2-τ-2θ_2-τ, where θ_2=2θ_1. The actual flip angle can then be determined from a ratio of the signals: $r = \sin^3\theta_1/\sin^3\theta_2$, which reduces to $r = 1/(2\cos\theta_1)^3$, where θ_1 is the actual flip angle[3].

A heating experiment was set up where a vile of canola oil and a vile of doped water (0.03g/l000ml magnesium sulfate) were heated outside of the scanner and then imaged as they cooled inside the scanner. Room temperature reference vials of oil and doped water were included to correct for field drift and fiber optic temperature probes were used to monitor the actual temperatures of all vials.

RESULTS

The image in the left of Fig. 1 shows the ratio of actual flip angle to expected flip angle for a vile of water. The actual flip angle can vary by +/-15%. The plot on the right of Fig.1 shows the difference between using data that was corrected for B1 inhomogeneities (red line) and data that was not (blue line) when calculating T1 values with this multi-flip angle technique.

Fig. 2 shows a plot of T1 versus temperature from a 4x4 voxel ROI near the temperature probe, with the mean and standard error displayed. Data from all three flip angles, 20°, 50°, and 70°, were used to calculate the T1 values. As expected, T1 values increase with increasing temperature. The change in T1 over the 20°C temperature change is in line with what others have reported (a change of ~1%/°C)[4].

Fig. 3 displays the PRF data, showing a plot of phase versus temperature. Again, a 4x4 voxel ROI near the temperature probe was taken and mean and standard error values are shown. While the data is very linear, the slope of -0.007 ppm/°C is slightly lower than the usually reported value of -0.01ppm/°C[1].

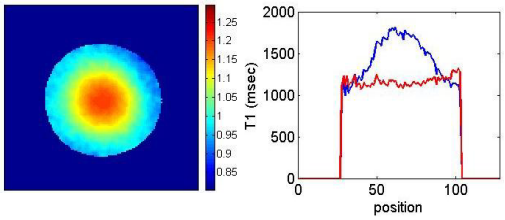

Fig. 1. *Left: Ratio of actual flip angle to expected flip angle. Right: Cross section of T1 values of water that have been corrected for B1 field inhomogeneities (red) and have not been corrected (blue).*

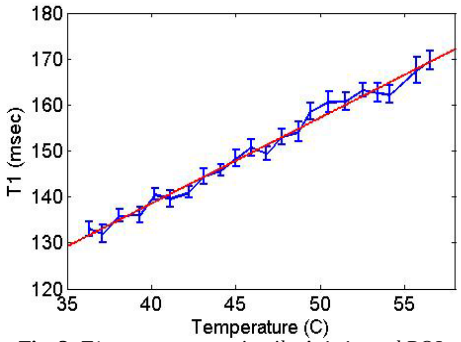

Fig. 2. *T1 vs temperature in oil. A 4x4 voxel ROI near the location of the temperature probe was considered, mean and standard error are displayed.*

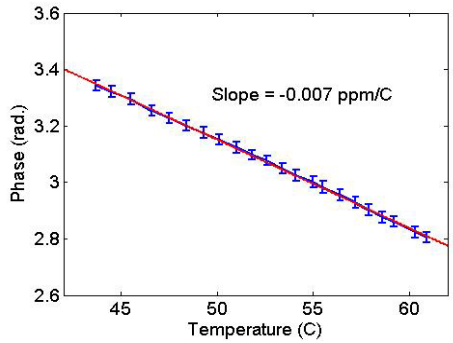

Fig. 3. *Phase vs temperature in water. A 4x4 ROI near the location of the temperature probe was considered, mean and standard error are displayed. The slope of -0.007ppm/°C is slightly lower than what is usually reported[1], but is within reason.*

CONCLUSIONS

We have demonstrated that a hybrid T1/PRF pulse sequence is capable of measuring those two temperature dependent parameters simultaneously. The use of a variable flip angle method to measure T1 allows the sequence TR to be held constant, and thus keeps scan time within the range needed for real time monitoring of thermal therapies. The next step will be to calibrate the T1 change as a function of temperature for various tissue types and apply the sequence to *ex vivo* tissues.

REFERENCES

1. J. De Poorter et al. MRM 1995 33(1), p.74-81.
2. S. Deoni et al. MRM 2003 49, p.515-526.
3. E.K. Insko et al. JMR 1993 103(A), p.82-85
4. B. Quesson et al JMRI 2000 12, p.525-533.

ACKNOWLEDGEMENTS: This work was supported by Siemens Medical Solutions, NIH F31 EB007892-01A1, and NIH R01 CA87785.